Article, Published Version

Lefebvre, Alice; Herrling, Gerald; Becker, Marius; Zorndt, Anna; Krämer, Knut; Winter, Christian

Morphology of estuarine bedforms, Weser Estuary, Germany

Earth Surface Processes and Landforms

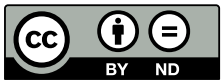

Received: 18 May 2021 | Revised: 3 September 2021 | Accepted: 7 September 2021

DOI: 10.1002/esp.5243

RESEARCH ARTICLE

ESPL WILEY

Morphology of estuarine bedforms, Weser Estuary, Germany

Alice Lefebvre[1] | Gerald Herrling[2] | Marius Becker[2] | Anna Zorndt[3] | Knut Krämer[2] | Christian Winter[2]

[1]MARUM, University of Bremen, Bremen, Germany

[2]Coastal Geology and Sedimentology, University of Kiel CAU, Kiel, Germany

[3]Federal Waterways Engineering and Research Institute (BAW), Hamburg, Germany

Correspondence
Alice Lefebvre, MARUM, University of Bremen, Bremen 28359, Germany.
Email: alefebvre@marum.de

Funding information
Deutsche Forschungsgemeinschaft, Grant/Award Number: 345915838

Abstract

Large bedforms (dunes) are present in many shallow-water environments. Knowledge of their dimensions and dynamics is required for river and coastal management. In tidal rivers and estuaries, the interaction among hydrodynamics (which results from the action of river and tidal flows), sediment transport and bedform shape and size is complex. In the present study, the distribution and morphology of bedforms in the Weser Estuary, Germany, were investigated. Bedforms were identified in bathymetric data of monthly multibeam echosounder surveys along the navigation channel during the years 2009 to 2013. Their size and shape were characterized. Bedforms were present along most of the channel, except at the position of the estuarine turbidity maximum and where dredging is carried out. Average bedform length varied between 20 and 60 m and bedform height between 0.3 and 1.6 m. Bedform asymmetry varied spatially and temporally along the estuary. In times of high river discharge, bedforms were generally more ebb-asymmetric than in times of low discharge. The bedforms were predominantly two-dimensional low-angle dunes with their steepest slope situated near the bedform crest. A significant proportion of bedforms possessed a steep face (portion of the lee side steeper than 15°). This implies that they are likely to create flow separation and a turbulent wake, with a strong potential to induce high bedform roughness. However, important variations in steep face area density were noted, both spatially along the estuary and temporally as a function of the tidal phase (ebb or flood) and the seasonal variation in river discharge. The results have wide implications in terms of understanding and modelling hydrodynamics and sediment transport in estuaries.

KEYWORDS
bedform shape, bedform size, data analysis, dunes, hydraulic roughness

1 | INTRODUCTION

Bedforms (ripples, dunes and sand waves) are ubiquitous features in sandy shallow-water environments. They exert a major influence on a range of processes, from small-scale turbulence and sediment transport to large-scale river and coastal geomorphology. For example, bedform size and shape are indicators of sedimentological and hydrodynamic conditions; the height and length of bedforms are commonly used to calculate bedform roughness; and navigation safety is ensured by limiting the height of bedform crests. Therefore, knowledge of the dimensions, morphological characteristics and dynamics of large bedforms is relevant for a wide range of fundamental and applied research. Bedform size, shape and dynamics are the result of their mutual interaction with the dominant hydrodynamic forcing: in rivers by unidirectional currents; in estuaries by reversing currents formed by the interaction between river and tidal flows; and in open marine environments by rotating tidal currents, waves and wind or wave-induced currents.

The interaction between flow and bedforms in unidirectional environments (rivers and flumes) has been studied intensively (see

reviews by Best, 2005; Venditti, 2013). Bedform size has been related to sediment properties, water depth and flow velocity (Southard & Boguchwal, 1990; Van Rijn, 1984). In laboratory flumes and small rivers, large asymmetrical angle-of-repose bedforms are formed, with a lee side of approximately 30° and a height generally larger than one-sixth of the water depth (Bradley & Venditti, 2017). Over such bedforms, the flow separates at the crest and recirculates over the steep lee side (Figure 1a, left panel). A turbulent wake develops along the shear layer between the separated and overlying flow, and dissipates downstream (Kwoll et al., 2016). Such bedforms generate a high bedform roughness several orders of magnitude larger than grain roughness (Van Rijn, 1984).

In large rivers, bedforms are mainly low-angle dunes with an average lee side slope of less than 10° (Cisneros et al., 2020). These bedforms are also smaller in height and length compared to the water depth than bedforms in small rivers (Bradley & Venditti, 2017). Due to the low-angle lee side slopes, there is little or no flow separation and turbulence over low-angle bedforms (Figure 1a, middle panel), and bedform roughness is small (Kwoll et al., 2016; Lefebvre & Winter, 2016). However, even over low-angle bedforms, parts of the lee side may still be steep enough to induce flow separation and generate a turbulent wake, and thereby produce an increase in shear stress compared to a flat bed (Lefebvre et al., 2016). Lefebvre (2019) suggested that the presence and size of reverse flow and turbulent wake are related to the characteristics of the lee side slope: if a portion of the slope is steeper than 15°, flow separation and increased turbulence are present (Figure 1a, right panel). Lefebvre (2019) defined this portion of the lee side steeper than 15° as a 'slip face', which is the name traditionally used by dune researchers to describe the steepest part of the lee side. However, the term 'slip' refers to the fact that sediment is sliding down or avalanching. Lefebvre (2019) analysed only how the steepness of the lee side may influence flow separation and turbulence but not sediment movement. Therefore, we use here the name 'steep face' to designate the portion of the lee side which is steeper than 15° and over which (intermittent) flow separation and a turbulent wake are produced. As shear stress over bedforms has been related directly to turbulence properties in the wake (Lefebvre et al., 2016), it is likely that the presence and characteristics of a steep face are good indicators of bedform roughness.

In tidal environments, flow reverses from one tidal phase to the next. Therefore, by definition, the positions of the stoss and lee sides switch during a tidal cycle (Figure 1b). Smaller (superimposed) bedforms often reverse their orientation and keep an asymmetry aligned with the flow, whereas larger bedforms stay oriented in one direction during the whole tidal cycle (Ernstsen et al., 2006b). The asymmetry of large bedforms, here defined as the relative length of the flood lee side, L_{fls}, compared to the bedform length, L (asymmetry $= L_{fls}/L$, Figure 1b), usually indicates the overall direction of bedform migration, and therefore the direction of residual sediment transport (Aliotta & Perillo, 1987; Barnard et al., 2011; Harris & Collins, 1984; Kubicki et al., 2017).

Bedforms have been observed in various estuaries around the world. Dalrymple and Rhodes (1995) give a thorough review of the early work related to estuarine bedform dynamics. Estuarine bedform

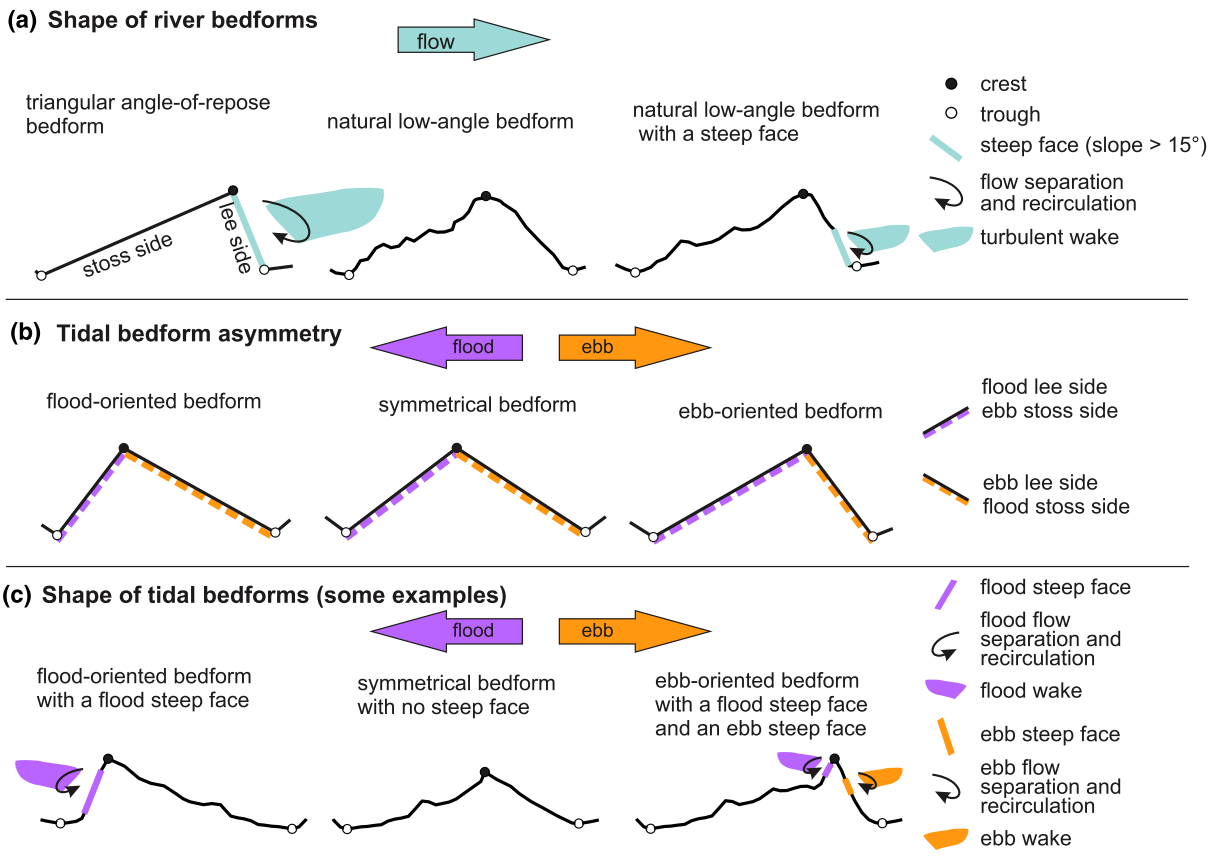

FIGURE 1 Definition of vocabulary used to describe river and tidal bedforms

size can be related to water depth, current speed, sediment grain size and sediment availability. The asymmetry of estuarine bedforms depends on various factors, notably the relative strengths of the flood and ebb currents and the size of the dune relative to the sediment transport rate (Dalrymple & Rhodes, 1995). In estuaries, the hydrodynamics result from a complex interaction between river discharge, which varies during the year, and tidal currents, which vary on various timescales (ebb and flood, spring and neap, longer astronomical timescales). Their interaction changes on a temporal scale, but also spatially along the estuary, especially through the propagation and deformation of the tidal wave and its interaction with the river flow. Bedform asymmetry and migration in estuaries has been observed to be influenced by river discharge, with an increase in ebb asymmetry and ebb-directed migration in times of high discharge compared to times of low discharge (Nasner, 1974; Zorndt et al., 2011). Similar to bedforms in large rivers, the shape of estuarine bedforms and its relation to flow direction is likely to control the presence of flow separation and a turbulent wake (Figure 1c), and ultimately bedform roughness.

The influence of bedform three-dimensional (3D) shape on the flow has been recognized since the early work of Allen (1968), and described based mostly on idealized bedforms in physical and numerical experiments (e.g. Lefebvre, 2019; Maddux et al., 2003; Venditti, 2007). However, the 3D shape of natural bedforms, especially natural large bedforms, has until now received little attention. Most methods to characterize dunes, even the most recent ones, still detect the bedform crest and trough in two dimensions (2D) from bed elevation profiles (BEPs) (Cisneros et al., 2020; Scheiber et al., 2021; Wang et al., 2020). Nowadays, high-resolution bathymetric data are widely available. It is therefore possible to study the 3D shape of bedforms.

Nasner (1974) has investigated the size and dynamics of dunes observed in the Weser Estuary, Germany, based on single-beam echosounder data collected in four reaches of the estuary. The dimension and migration of the measured dunes (average height ca. 2 m) were found to be related to tidal currents and water discharge. Recently, Herrling et al. (2021) estimated the effect of asymmetric dune roughness on tidal asymmetry in the Weser Estuary. Based on numerical simulation results, they showed that the spatio-temporal interaction of distinct dune shapes with the main drivers of estuarine sediment and morphodynamics (river discharge and tidal energy) is substantial. They highlighted the need to consider dune-induced directional bed roughness in numerical models of estuarine and tidal environments. To do so, estimates of dune size and asymmetry are needed.

This study aims to investigate the shape and dynamics of large bedforms (dunes) in the Weser Estuary. In particular, the variations of bedform properties, both spatially along the estuary and in times of high or low river discharge, are examined. The properties investigated are the bedform height, length and asymmetry, and their morphology, notably the lee side shape (e.g. presence and position of steep lee slopes) and 3D characteristics (e.g. crestline shape). With this, we aim to: (1) describe bedform presence and morphology along the Weser Estuary; (2) identify the differences between the morphology of river and estuarine bedforms; and (3) estimate the potential for bedforms in the Weser Estuary to influence flow properties.

2 | METHOD AND STUDY AREA

2.1 | Weser Estuary

The Weser is a 452 km-long river which flows in north-western Germany and discharges into the German Bight, southern North Sea (Figure 2). Between the tidal barrier in Bremen (Weser-km −5) and the mouth of the estuary (Weser-km 112), the Weser is influenced by the tides. The official kilometrage of the Weser Estuary starts at Bremen Weserbrücke (km 0), 5 km downstream of the tidal barrier. The estuarine reach can be subdivided into the Lower Weser (Bremen to Bremerhaven, km −5 to 67) and the Outer Weser downstream from Bremerhaven to the open North Sea. The Lower Weser has been substantially engineered during the 19th and 20th centuries (Kunz, 1994): between 1888 and 1895, the 'Weser correction', planned by Ludwig Franzius (Franzius, 1888), straightened the waterway and cut off secondary channels in order to concentrate and intensify tidal and river flows. Until 1999, several deepenings and widenings of the main channel were carried out to enhance ship traffic between the North Sea and Bremen, resulting in an increase of the mean tidal range in Bremen from a few decimetres in 1900 to over 4 m nowadays. At the Outer Weser, several channel–shoal systems with large intertidal areas drain into the estuarine channel. The Weser Estuary can be classified as partially mixed (Grabemann et al., 1997). The mixing zone position varies with river discharge: between Weser-km 52 and 73 during low and high discharge, with an average position around Weser-km 57 in average runoff conditions (Zorndt & Schlurmann, 2014). The estuary is characterized as mesotidal, with a mean tidal range increasing upstream from 2.9 m at the mouth (Weser-km 112) to a maximum of 4.2 m in Bremen (Weser-km 0, Figure 2b). The mean water depth along the navigation channel increases from approximately 6 m in Bremen to up to 22 m at the Outer Weser (Figure 2c). The engineered fairway channel has an almost constant width of 200 m between Bremen and the port of Brake (Weser-km 39), then expands gradually towards the North Sea (Figure 2d). The channel bed is characterized by medium to coarse sands with locally large amounts of cohesive sediments (Figure 2e). An estuarine turbidity maximum (ETM), around 20 km in length, is found in the region between Weser-km 50 (low river discharge) and 75 (high river discharge), with a maximum suspended sediment concentration of 400 to 700 mg/L (Grabemann & Krause, 2001). The cohesive sediment content in the main channel is largely below 25% except for local peaks of 50–75% along the port of Bremen (Weser-km 5 to 8) and at the ETM (Figure 2e). Long-term (1990–2010) minimum, mean and maximum river discharge measured at Intschede in the riverine part upstream of the tidal barrier are 116, 324 and 1220 m^3/s, respectively.

The Weser Estuary is an important waterway connecting the ports of Bremen and Bremerhaven to the North Sea. To guarantee access for the large ships navigating the estuary, the channel depth is periodically monitored by the responsible authorities and water depth is maintained. Between Weser-km 8 and 55, where sandy sediments and bedforms dominate, water injection is used locally to mobilize the material on the dune crests so that it settles in dune troughs in the vicinity (Nasner et al., 2009). In the ETM and the Outer Weser,

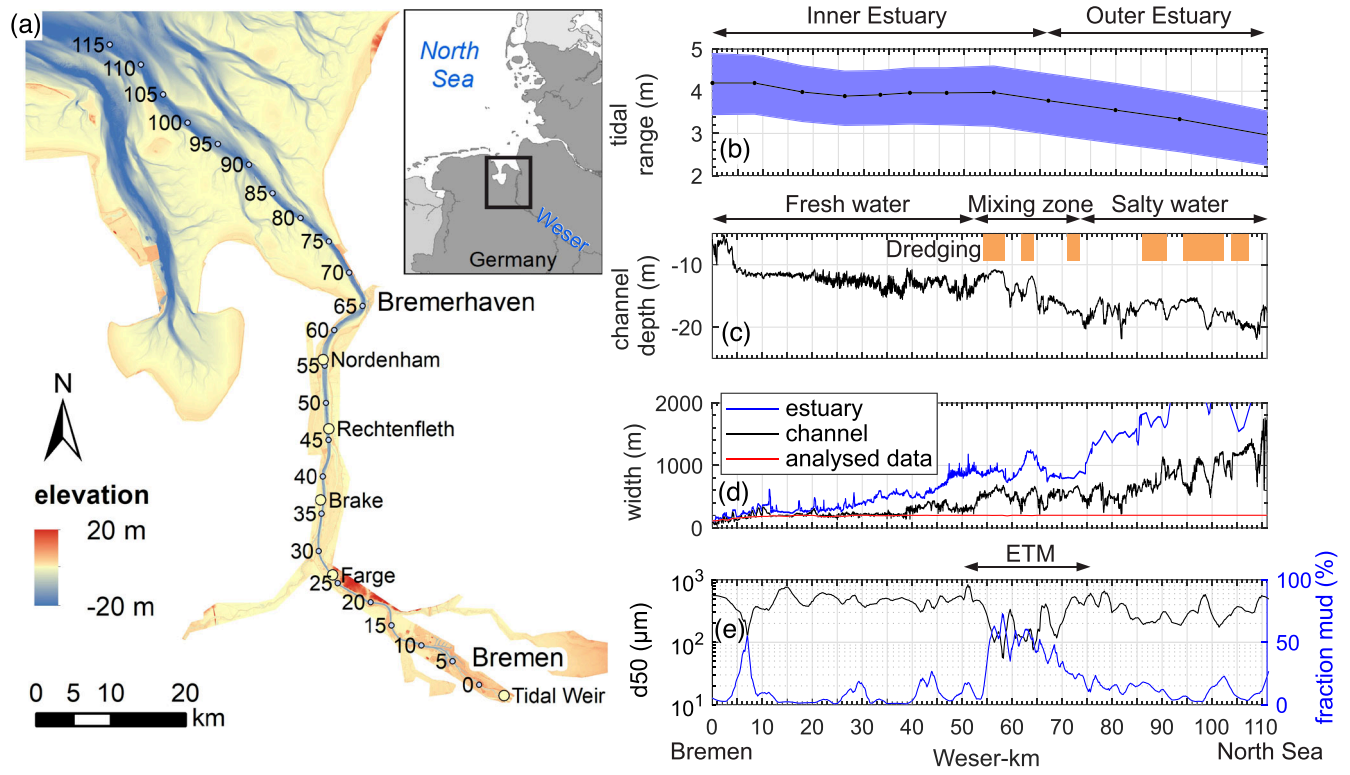

FIGURE 2 (a) The Weser Estuary in the southern North Sea, Germany; (b) mean tidal range (black line) and mean spring tidal ranges (blue fill); (c) depth of the navigation channel (the filled orange rectangles show areas with frequent maintenance dredging); (d) width of the estuary, navigation channel and analysed data; and (e) median grain diameter (d_{50}) and mud fraction along the navigation channel (note the position of the ETM around Weser-km 55 to 75)

dredging is conducted to maintain the water depth (Figure 2c). Dredged sediment is deposited at dumping sites on the side of the channel in the Outer Weser.

2.2 | Analysed data

The navigation channel of the Weser Estuary is surveyed on a nearly monthly basis by the Weser–Jade–Nordsee Waterways and Shipping Authorities (Wasserstraßen- und Schifffahrtsamt Weser-Jade-Nordsee WSA WJN) by means of multibeam echosounder (MBES). Gridded data with a cell size of 2 × 2 m were made available by WSA WJN along the main waterway between Weser-km 0.0 and 110 for the years 2009 to 2013 (Figure 3). It should be noted that due to the relatively coarse grid size, only the large bedforms (>10 m long) were examined. It is likely that smaller bedforms are found superimposed on the large ones, but the data resolution did not allow us to investigate them.

The river discharge is recorded daily in Intschede, around 25 km upstream of the weir in Bremen, and is freely available online (Flussgebietsgemeinschaft Weser, n.d.). The river discharge during the study period, Q, is plotted in Figure 3a. In order to characterize bedform properties in times of high and low discharge, we differentiate between times when $Q > 350$ m^3/s (high discharge, in winter and spring) and when $Q < 200$ m^3/s (low discharge, in summer and autumn).

2.3 | Bedform detection

The processing applied in the bathymetric data is shown as a flowchart in Figure 4 and in detail in Supporting Information 1. Over 1200 raw files were analysed over the 5-year period (Figure 3b). The data were first projected from DHDN3 into ETRS 1989 UTM coordinate system, keeping the 2 m grid resolution. The data were then interpolated onto a curvilinear grid specifically created for this study. The centreline of the curvilinear grid follows the official waterway position, in the middle of the navigation channel (given by the Federal Waterway Network, n.d.). To create the curvilinear grid, the waterway centreline was interpolated on a regular 2 m spacing. The coordinates of points perpendicular to the waterway were then calculated every 2 m in the cross-stream direction. In places of strong curvature, a constant 2 m grid in both streamwise and crosswise directions cannot be ensured as it could lead to overlapping sections on the inner side of the curve. The 2 m resolution was maintained over the centreline and some smaller (larger) spacing were allowed in the inner (outer) bends away from the centreline (over the whole grid, average resolution of 2.00 m, standard deviation of 0.04 m).

The method applied to analyse the data is described here briefly and in detail in Supporting Information 1. Importantly, we aimed at characterizing the 3D bedform morphology, thus a new method was developed to detect crest and trough lines and not just crest and trough points. Following Ogor (2018), raw crestlines were detected from the projected 3D bathymetry as objects with a minimum

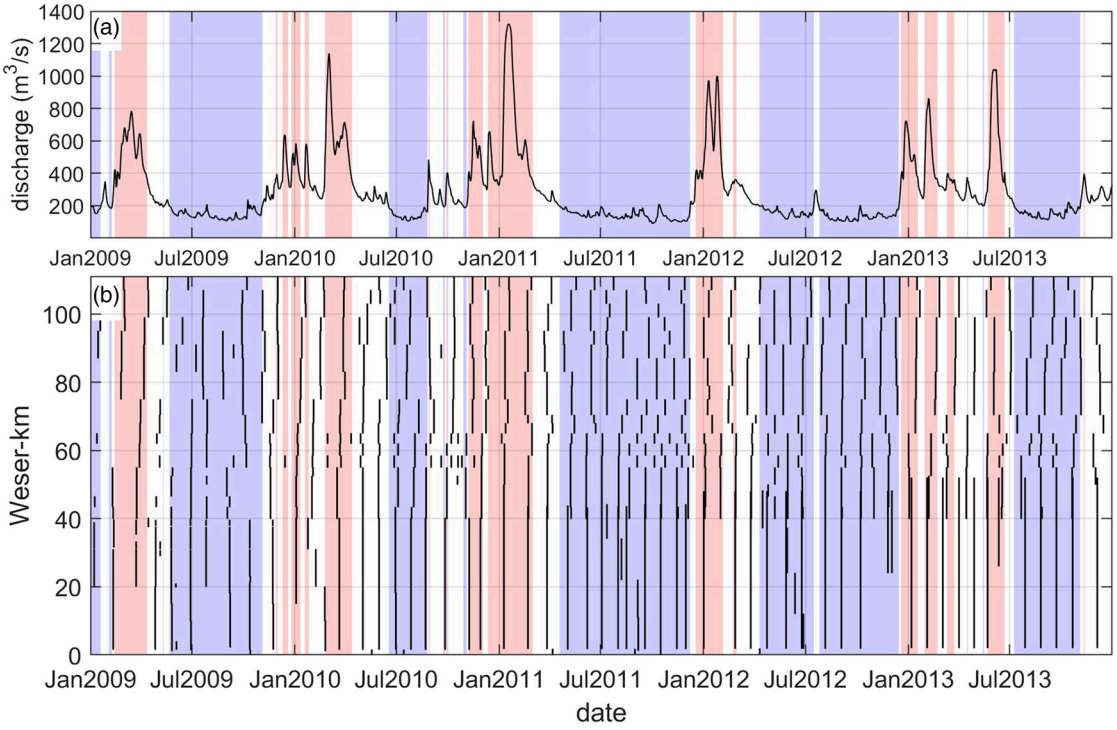

FIGURE 3 (a) River discharge during the study period. Times of high discharge (discharge > 350 m^3/s) are highlighted by a pink background and times of low discharge (discharge < 200 m^3/s) are highlighted by a blue background; (b) temporal and spatial extent of available files (each line represents a 2-m gridded bathymetry along the waterway)

curvature lower than a threshold. To do so, the minimum curvature was calculated from the 3D bathymetry. Crest points were found as minimum curvature smaller than a threshold of $-0.04\ m^{-1}$. Image analysis techniques applied on these raw crestline points allowed the determination of crestlines consisting of connected points. Trough points were found as minimum elevation between crestlines on bed elevation profiles taken through the curvilinear grid. Image analysis applied on the trough points allowed the determination of trough lines consisting of connected points. In order to assess the crestline three-dimensionality, the length of each crestline was calculated. The orientation of each of the crestline points was determined as the angle between a line formed by the crestline point and its crosswise neighbour, and the waterway direction.

The steep faces were determined on the 3D bathymetry from the slope angle magnitude and direction as portions of the slopes containing at least four points (in the streamwise or crosswise direction) with angles steeper than 15° and a direction within ±45° of the streamwise direction. In order to calculate the steep face orientation, each steep face was represented by a line calculated by fitting a smoothing spline through each steep slope (see Supporting Information 1 for details). The orientation of each point of the steep face line was calculated as the angle between the steep face line and the waterway direction.

Following the estimation of 3D characteristics, individual measurements of bedform properties were performed on BEPs; specifically, a 'BEP bedform' was defined as a bed elevation profile portion along which a trough was followed by a crest and a trough. From this BEP bedform, bedform length and height, height and length of ebb and flood lee sides, bedform asymmetry (length of flood lee side/bedform length), mean and maximum angle of the ebb and flood lee side angle, horizontal and vertical position of the maximum angle of the flood and ebb lee side, presence and position of ebb and flood steep faces were calculated (see details in Supporting Information 1).

Bedform characteristics were then averaged over 1 km-long sections. Before this, erroneous measurements (e.g. bedforms with a negative height) were discarded (5.6% of the measurements). Bedforms longer than 200 m or higher than 4 m, as well as bedforms smaller than 10 m in length or 0.2 m in height, were also removed from the analysis (1.4 and 1.8% of the measurements, respectively). Along each section, the BEP bedform density was calculated as the number of BEP bedforms per square kilometre. This number is a way to quantify dune density, however, it does not reflect the actual number of dunes, as each dune is measured several times along the cross-stream direction. The crestline density was calculated as the number of crestlines per square kilometre. This actually represents the number of bedforms. Finally, the steep face area density was calculated as the area of steep faces (width * height * angle) per square kilometre. It should be noted that the crestline density and the steep face area density do not rely on the BEP analysis to be calculated. They are calculated from the 3D bathymetry.

The data were subsequently averaged in time, over the whole time period (around 50 files for each kilometre-long section), at times of high discharge when the discharge was more than 350 m^3/s (Figure 3, around 10 files for each kilometre-long section) and at times of low discharge when the discharge was less than 200 m^3/s (around 30 files for each kilometre-long section).

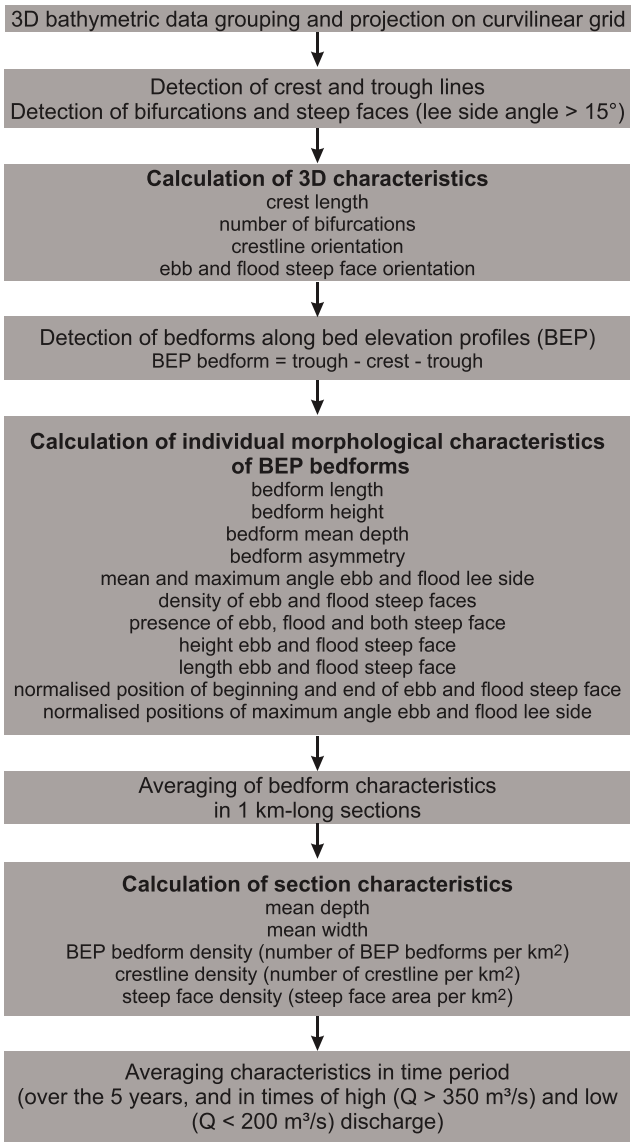

FIGURE 4 Flowchart of the processing applied on the available data

3 | RESULTS

3.1 | Time-averaged bedform properties

Bedform characteristics averaged over the 5-year study period are shown in Figures 5, 6 and 7. Summary and histograms of bedform properties are also given in Supporting Information 2. Generally, over the whole estuary, three bedform fields can be recognized by high BEP bedform and crestline densities, separated by two regions where no or few bedforms are found (Figure 5b). Bedform Field 1 (Weser-km 13 to 54) has the highest number of bedforms measured, with maximum crestline density of 587 crestlines/km^2 at Weser-km 20 and maximum BEP bedform density of 12 600 bedforms/km^2 at Weser-km 28 (Figure 5b). Only a few bedforms (on average 43 crestlines/km^2) are found in the ETM (Weser-km 55 to 72). Bedform Field 2 (Weser-km 73 to 84) has generally a low BEP bedform density (on average 130 crestlines/km^2), except around Weser-km 75. Between Weser-km 85 and 98, regular dredging takes place and no bedforms are observed. Finally, some bedforms (on average 66 crestlines/km^2) are found along Bedform Field 3 (Weser-km 99 to 110).

Bedform length generally increases along the Weser Estuary, with an average value of around 40 m in the upstream part of Bedform Field 1, rising to 70 m in the North Sea (Figure 5c). Bedform height also generally increases along the estuary, with a bedform height of around 0.7 m towards Bremen, and a maximum value of 2 m at Weser-km 106 (Figure 5d). The mean bedform height/length ratio is on average 0.03 along the whole estuary and varies between 0.02 and 0.06. The height/length ratio is highest between Weser-km 25 and 35, which is also where the highest bedform density is found.

Most remarkably, bedform asymmetry varies substantially along the estuary (Figure 5f). Near Bremen, the bedforms are on average flood-asymmetric (i.e. their flood lee side is shorter than their ebb lee side). Between Weser-km 16 and 30, they are on average symmetrical. Downstream of Weser-km 30, their ebb asymmetry increases until the end of Bedform Field 1. Along Bedform Field 2, the bedforms are on average symmetrical. In Bedform Field 3, they are predominantly ebb-asymmetric.

The mean ebb and flood lee side angles are on average only 6.1 and 4.7°, and the maximum ebb and flood lee side angles are on average 11.6 and 10.0° (Figures 5g and h). Therefore, bedforms in the Weser Estuary are overall low-angle dunes. The flood lee side angles do not show strong coherent variations along the estuary. In contrast, the ebb lee side angles distinctly increase along Bedform Field 1, which agrees with the observed increase in ebb asymmetry. In other words, as the bedforms are getting more ebb-asymmetric, their ebb lee side angle is getting steeper.

In order to better understand how the bedforms in the Weser Estuary interact with the flow, steep face (portion of the lee slope steeper than 15°) characteristics were calculated. The steep face area density has very different values for the ebb and flood lee sides (Figures 6a and b). In the upstream part of Bedform Field 1 (until ca. Weser-km 20), the steep face area density is 1480 m^2/km^2 during the flood but only 35 m^2/km^2 during the ebb. Downstream of Weser-km 20 and along the remainder of Bedform Field 1, ebb steep face density stays high with an average of 26 530 m^2/km^2. Between Weser-km 20 and 35, flood steep face density is on average 9240 m^2/km^2 and decreases to 2150 m^2/km^2 downstream of Weser-km 35. Along Bedform Fields 2 and 3, steep face densities are low (around 2000 m^2/km^2), apart from at Weser-km 75.

When examining the relative presence of steep faces (Figure 6c), it can be noted that the steep face presence roughly follows bedform asymmetry. The highest density of steep faces is found between Weser-km 21 and 54. There, around 25–60% of the bedforms possess a steep face. Interestingly, up to 8% of the bedforms in this region have a steep face on both their ebb and flood sides (morphology as exemplified in Figure 1c, right panel).

Lefebvre (2019) suggested that flow separation and turbulent wake sizes were related not only to the presence of a steep face, but also to steep face height. Along the Weser Estuary, the ebb steep face height follows roughly the variations in bedform height within Bedform Field 1 (Figure 6d). However, in Bedform Fields 2 and 3, the steep face height is relatively constant whereas the bedform height is increasing. The flood steep face height shows little variation along the estuary, it is around 0.8 m in Bedform Field 1 and around 1 m in Bedform Field 2 (Figure 6f).

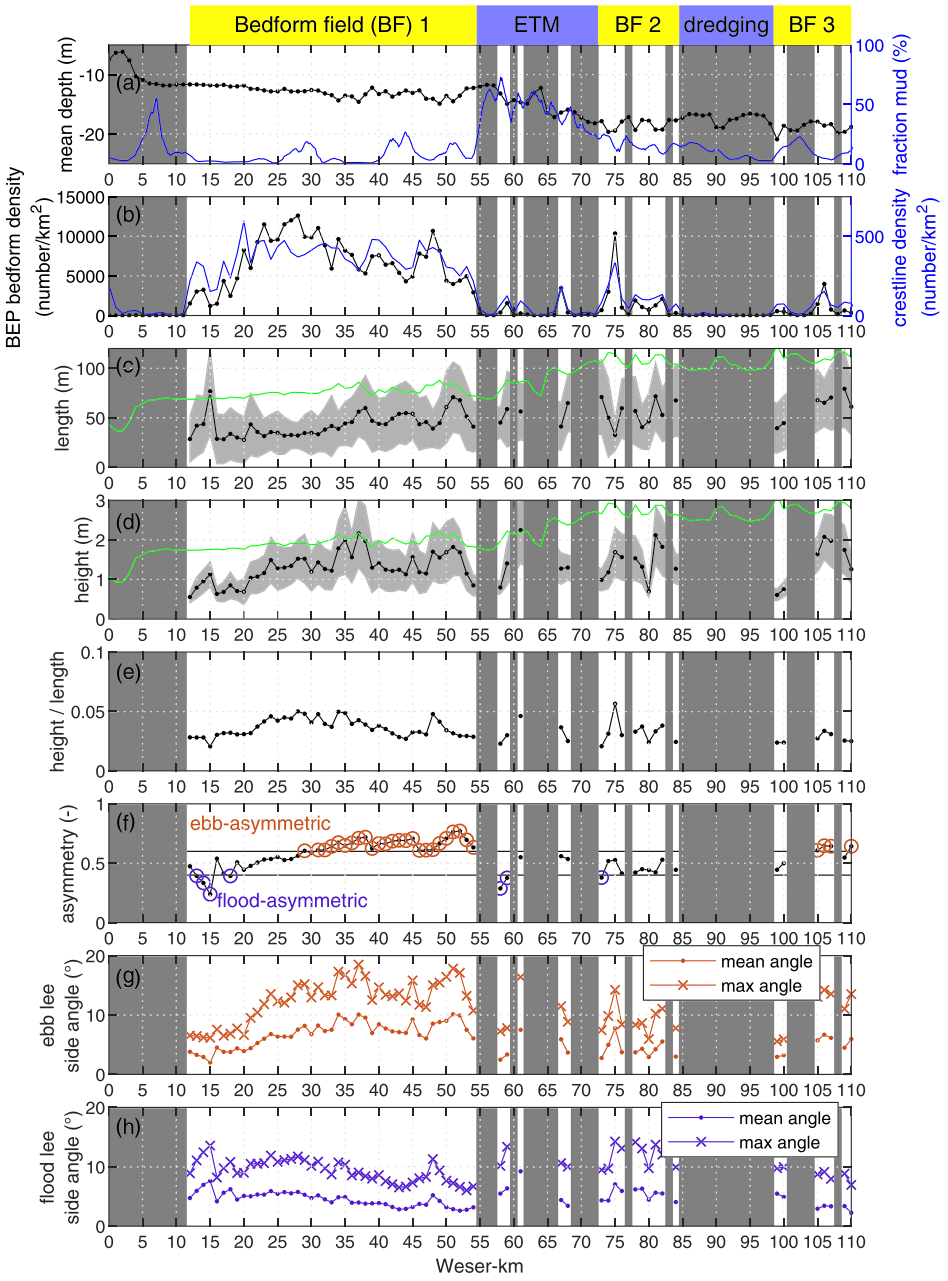

FIGURE 5 Bedform characteristics along the Weser Estuary averaged over the 5-year study period: (a) mean depth and mud fraction; (b) BEP bedform density (black) and crestline density (blue); (c) mean bedform length (black) and standard deviation (grey), and scaling relation between length and depth proposed by Bradley and Venditti (2017), length = 5.9 × depth (green); (d) mean bedform height (black) and standard deviation (grey), and scaling relation between height and depth of field bedforms proposed by Bradley and Venditti (2017), height = depth/6.7 (green); (e) height/length; (f) asymmetry, mean asymmetry < 0.4 (flood-asymmetric--asymmetric bedform field) is highlighted with violet circles, mean asymmetry > 0.6 (ebb-asymmetric bedform field) is highlighted with orange circles; (g) ebb lee side mean and maximum angle; (e) flood lee side mean and maximum angle. The grey background on all plots shows the region where hardly any bedforms are found (BEP bedform density < 250 bedforms/km^2)

The vertical and horizontal positions of the maximum slope of the lee side (Figures 6f and g), as well as the position of steep faces (Figure 6h), can be used to estimate the lee side shape (see Figure 1 and Supporting Information 1). Note that the vertical position of the maximum slope (vertical distance between the trough and the maximum angle, H_{ma}, with respect to the lee side height, H_{ls}, see Supporting Information 1 for details) is similar to the fractional height of the maximum lee side slope calculated by Cisneros et al. (2020). The maximum slope of the Weser bedforms is generally positioned between 0.5 and 0.7 H_{ma}/H_{ls}, with average values of 0.60 and 0.64 H_{ma}/H_{ls} for the ebb and flood lee sides, respectively. This means that the maximum angle is found on the upper part of the lee side, closer to the crest than to the trough. The horizontal position also confirms that the maximum slope is generally located close to the crest, between 0.2 and 0.5 L_{ma}/L_{ls} (where L_{ma} is the horizontal distance between the crest and the maximum angle and L_{ls} is the lee side length), and on average at one-third of the distance between the crest and the following trough (Figures 6g and h). Interestingly, when a steep face is present, the maximum slope is generally closer to the crest (0.30 and 0.33 L_{ma}/L_{ls} for the ebb and flood lee side, respectively) than on average (0.31 and 0.35 L_{ma}/L_{ls} for the ebb and flood lee side, respectively). The ebb and flood steep faces are both close to the crest, situated at 0.11–0.38 and 0.19–0.39 from the crest, respectively.

Several parameters were calculated to assess the bedform three-dimensionality along the estuary (Figure 7). It should be noted that the width of the channel varies along the estuary: near Bremen, the channel is comparatively narrow (ca. 90 m); between Weser-km 10 and 38, the channel width stays relatively constant (200 m); downstream of Weser-km 38, the channel width increases gradually from 300 m to over 1000 m (Figure 2c). However, the data which were analysed had a constant maximum width of 200 m. Therefore, the present analysis considers only the bedforms found in the centre of the channel. Due to secondary currents and other channel curvature effects, hydrodynamics and sediment transport are likely to be variable over the channel cross-section. Therefore, the bedform

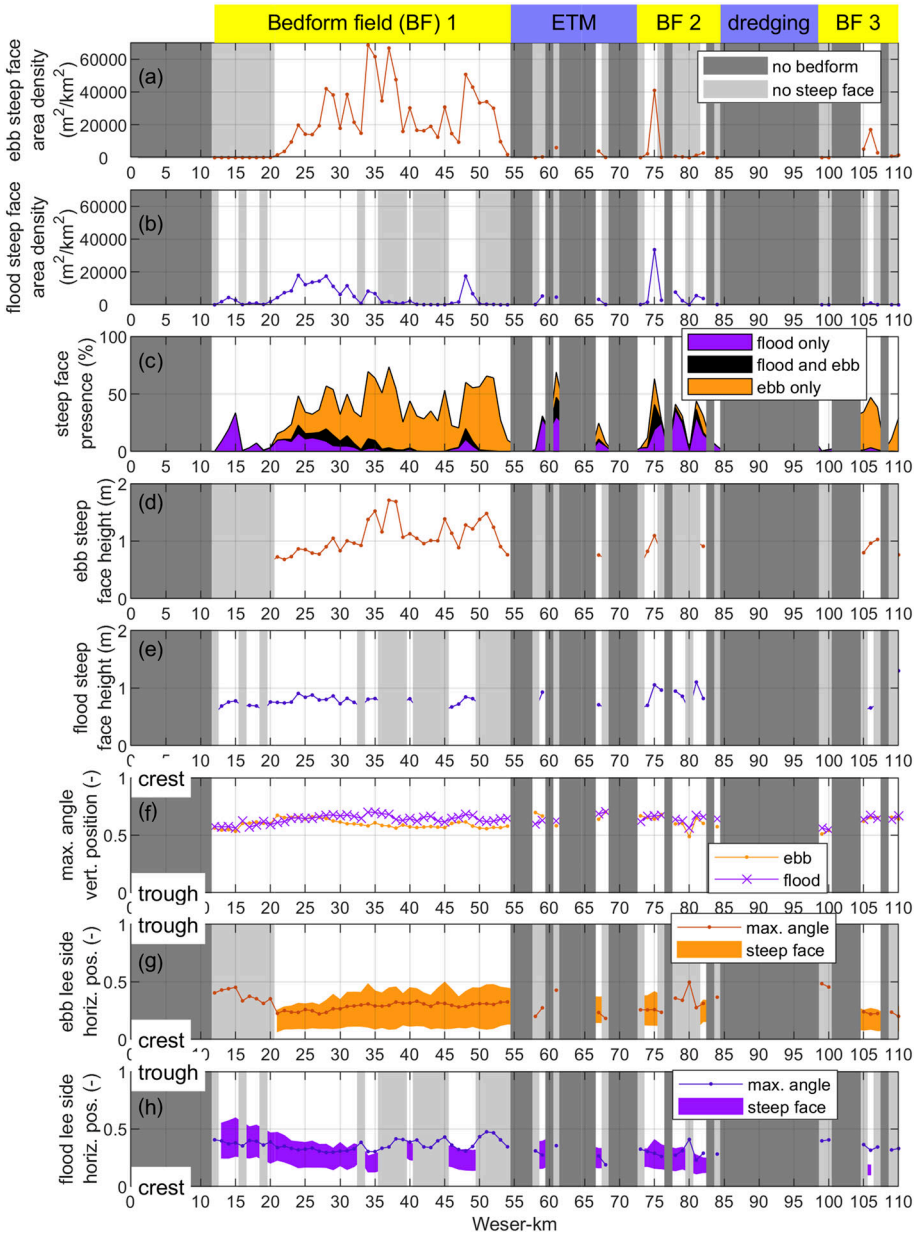

FIGURE 6 Bedform characteristics along the Weser Estuary averaged over the 5-year study period: (a) ebb steep face area density; (b) flood steep face area density; (c) percentage of BEP bedforms (compared to the total number of BEP bedforms measured) which possess a flood steep face, an ebb steep face, or both a flood and ebb steep face; (d) ebb steep face height; (e) flood steep face height; (f) vertical position (between the trough and the crest) of the lee side maximum angle; (g) horizontal position (between the crest and the trough) of the ebb lee side maximum angle (solid line) and horizontal position of the ebb steep face (fill); (h) horizontal position (between the crest and the trough) of the flood lee side maximum angle (solid line) and horizontal position of the flood steep face (fill). The dark grey background on all plots shows the region where hardly any bedforms are found (BEP bedform density < 250 bedforms/km^2)

morphology analysed in the Outer Weser (especially after Weser-km 38) may not be representative of the dynamics of the whole channel. The crest length is on average 50 m, which means that the crests extend on average along one-quarter of the measured channel width (200 m). At the beginning of Bedform Field 1, the average crest length is 25 m and it increases downstream to a maximum of 85 m at Weser-km 28. Along Bedform Fields 2 and 3, the crest length is variable (between 25 and 94 m).

The number of bifurcations with respect to the number of crestlines is on average 0.25 over the estuary, meaning that one in four crestlines has a bifurcation. However, this number also includes the very small crests (<4 points), which were then discarded for analysis. Therefore, the number of bifurcations should not be taken as an absolute number but to assess qualitatively the variations in bifurcation number along the estuary. The number of bifurcations is generally higher along Bedform Field 1 (mean value of 0.29) compared to Bedform Fields 2 and 3 (mean value of 0.14).

The crestlines have an average orientation of 2.8° anti-clockwise compared to the waterway orientation, with a mean standard deviation of 25.5° and no obvious trend along the estuary (Figure 7d). The ebb and flood steep faces are overall oriented perpendicular to the waterway, with average orientations of 0.9 and 0.6° (Figures 7f and g). Overall, the Weser bedforms appear to be 2D with no clear trend in any of the indicators of three-dimensionality along the estuary.

3.2 | High and low discharge

Bedform characteristics were calculated for records of what is referred to as 'high discharge' and 'low discharge' (respectively, river discharge > 350 m^3/s and river discharge < 200 m^3/s; see Figure 3). In the present work, seasonal variations (i.e. high discharge vs low discharge) are investigated in order to characterize the range of bedform shapes which may be found in the Weser Estuary. This work does not examine the reaction time of bedform characteristics to hydrodynamic variations. That is why bedform characteristics are averaged during periods of low and high discharge and not plotted directly against

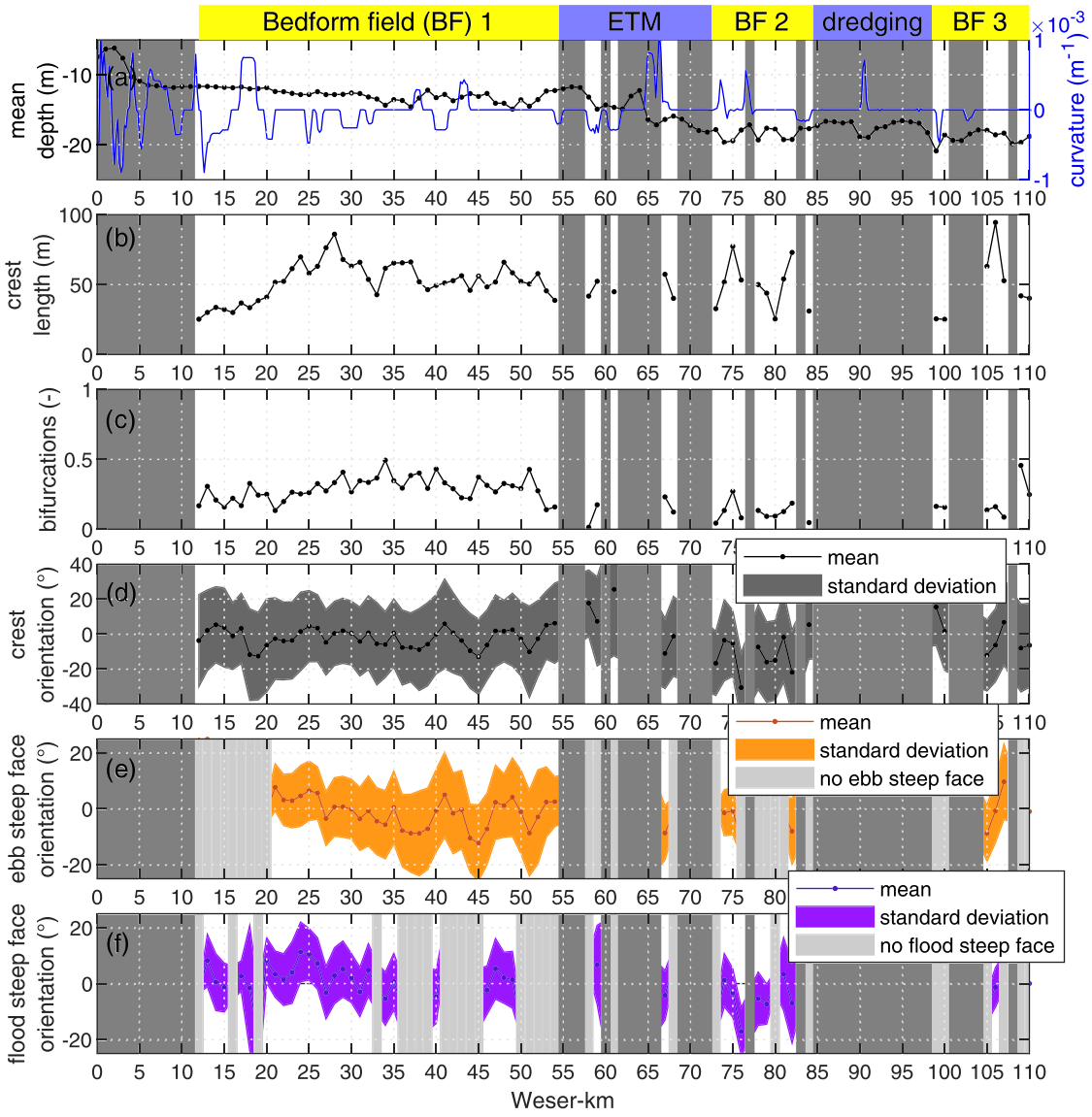

FIGURE 7 Bedform characteristics along the Weser Estuary averaged over the 5-year study period: (a) mean depth and curvature; (b) crest length; (c) number of bifurcations divided by the number of bedform crests; (d) crest orientation compared to the waterway direction, the grey fill around the solid line shows the standard deviation of crest orientation; (e) ebb steep face orientation compared to the waterway direction, the grey fill around the solid line shows the standard deviation of ebb steep face orientation; (f) flood steep face orientation compared to the waterway direction, the grey fill around the solid line shows the standard deviation of flood steep face orientation. The dark grey background on all plots shows the region where hardly any bedforms are found (BEP bedform density < 250 bedforms/km^2)

river discharge. The discharge conditions chosen for the averaging were taken to allow a sufficient number of data for averaging and exclude measurements taken during intermediate discharge, when bedforms may still be adapting to previous discharge conditions and may present transitional shapes.

The characteristics showing the most differences depending on discharge are presented in Figure 8. The bedforms in the three bedform fields reacted differently to discharge. In Bedform Field 1, bedform height is not substantially affected by discharge, but the bedforms are longer, and therefore feature a lower height/length ratio, in times of high discharge compared to times of low discharge (Figures 8c–e). Importantly, the bedforms are systematically more ebb-asymmetric in times of high discharge compared to times of low discharge (Figure 8f). The mean ebb lee side angle is consistently steeper, and the mean flood lee side angle gentler in times of high discharge compared to times of low discharge (Figures 8g and h). In addition, in times of high discharge, nearly no bedform is found with a flood steep face, whereas a large proportion of bedform possesses an ebb steep face (Figure 9). In times of low discharge, in contrast, a transition is seen between Weser-km 12 to 22, where bedforms with a flood steep face are found, Weser-km 22 to 35, where bedforms with flood, ebb or both ebb and flood steep faces are detected, and Weser-km 35 to 55, where bedforms with ebb steep faces are observed.

In Bedform Field 2, bedform characteristics do not vary strongly depending on discharge. No systematic trend is observed regarding bedform height and length, symmetry, lee side angles or steep face density, depending on times of low or high discharge.

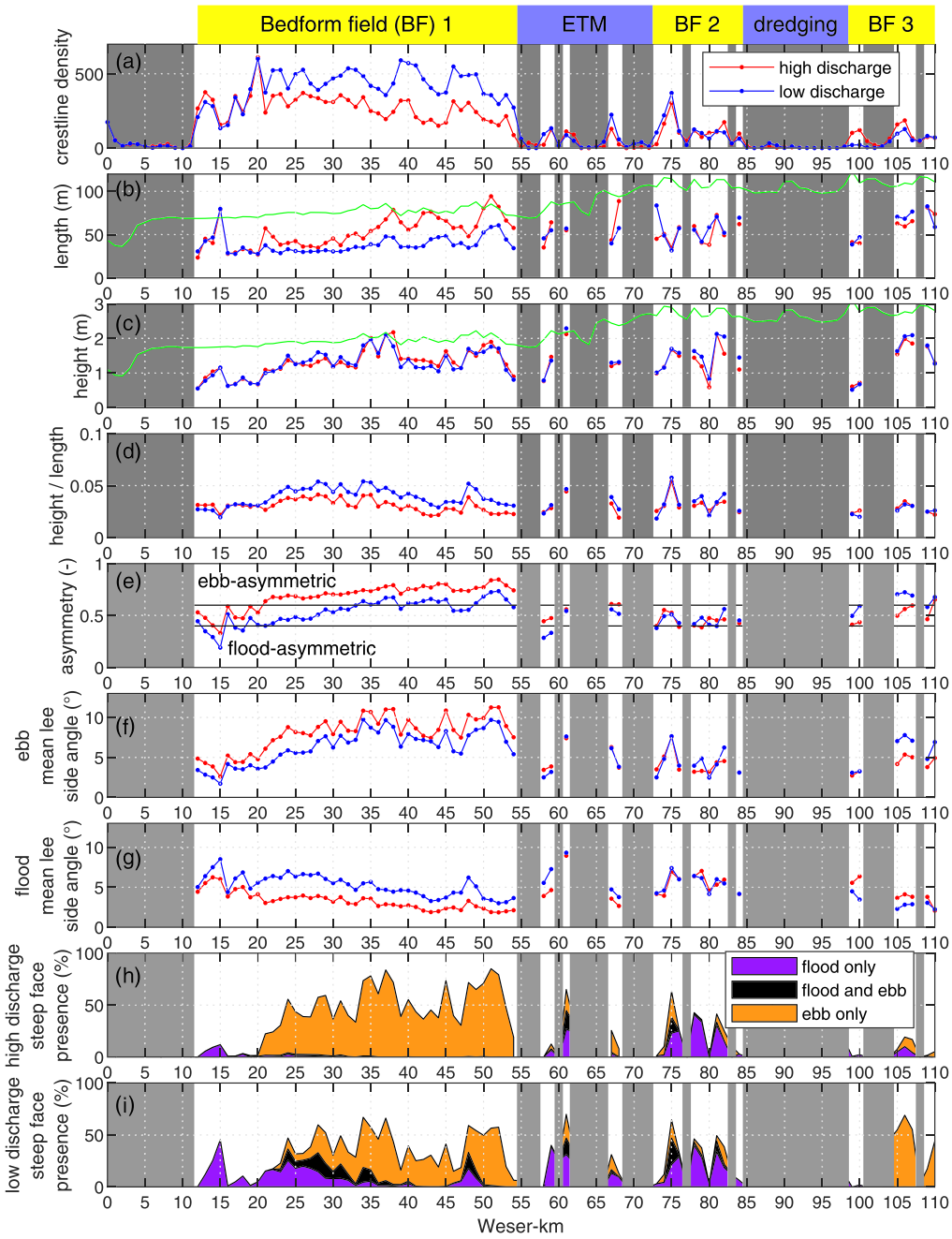

FIGURE 8 Bedform characteristics along the Weser Estuary averaged in times of high discharge (red) and low discharge (blue): (a) crestline density (number of crestlines per square kilometre); (b) bedform length and scaling relation between length and depth proposed by Bradley and Venditti (2017), length = 5.9 × depth (in green); (c) bedform height and scaling relation between height and depth of field bedforms proposed by Bradley and Venditti (2017), height = depth/6.7 (in green); (d) height/length; (e) asymmetry; (f) ebb lee side mean angle; (g) flood lee side mean angle; (h) percentage of bedforms (compared to the total number of bedforms measured) in times of high discharge which possess a flood steep face, an ebb steep face, or both a flood and ebb steep face; (i) percentage of bedforms (compared to the total number of bedforms measured) in times of low discharge which possess a flood steep face, an ebb steep face, or both a flood and ebb steep face. The grey background shows the region where hardly any bedforms are found

In Bedform Field 3 (in the Outer Weser), height and length are not consistently affected by discharge, so the height/length ratio does not vary much with discharge. Bedforms are generally symmetric in times of high discharge, and ebb-asymmetric in times of low discharge, i.e. showing a behaviour contrary to that observed in Bedform Field 1. In addition, in times of low discharge, only ebb steep faces are observed, whereas a small number of ebb and flood steep faces are found in times of high discharge.

4 | DISCUSSION

4.1 | Variations of tidal bedform properties in time and space

Tidal bedform properties in the Weser Estuary were found to vary spatially and temporally along the estuary. On the scale of the estuary, large bedforms are observed starting from Weser-km 12. Upstream of

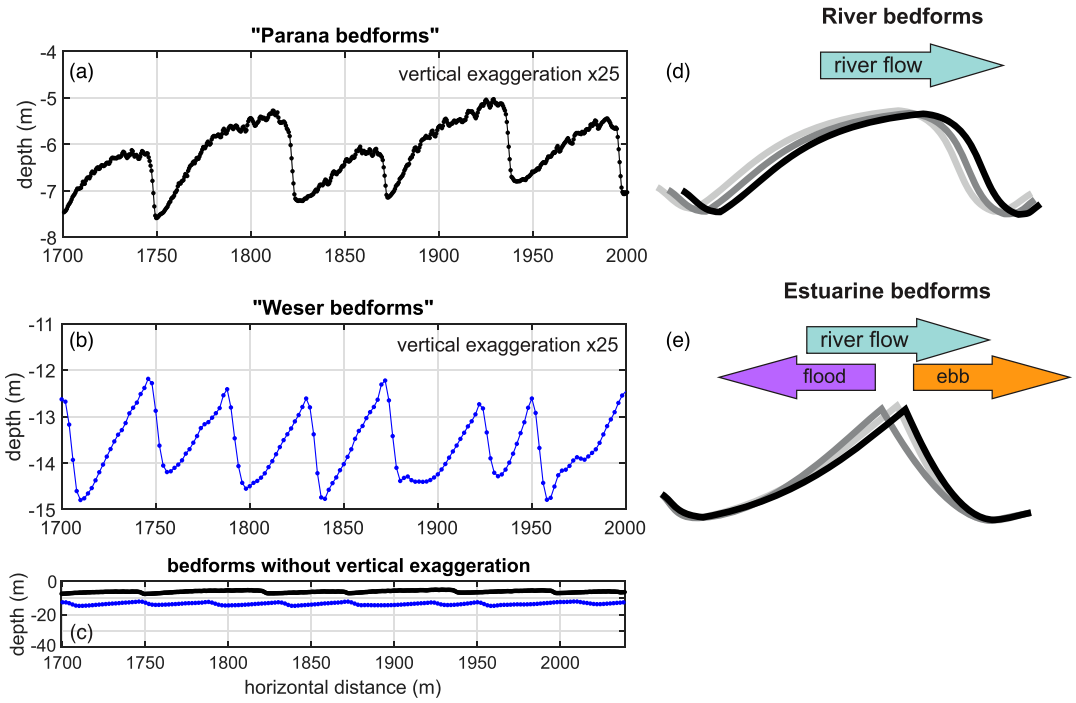

FIGURE 9 Bathymetric profiles from (a) the Parana River (data from Parsons et al., 2005) and (b) the Weser Estuary to highlight the differences in bedform morphology; (c) profiles of the Weser and Parana bedforms presented without vertical exaggeration and schematic representation of transport processes on a short timescale (e.g. tidal cycle) which may explain the distinctive shape of estuarine and river bedforms: (d) in rivers, the crest is constantly being eroded and the sediment deposited over the lower lee side, forming a flat crest and steep lower lee side; (e) in estuaries, sediment is being moved back and forth over the crest by the tidal currents with little net movement, forming bedforms with sharp crests and flat troughs

this, only a few bedforms with low aspect ratio (mean height/length = 0.08) are detected. This is probably due to a combination of weak hydrodynamics near the tidal barrier and local high mud content (Figure 2), which restricts the formation of large bedforms near Bremen. Between Weser-km 12 and 55, the largest bedform field of the Weser Estuary is observed. Between Weser-km 55 and ca. 62, only a few bedforms were found in the so-called Weser mud reach, where bed sediments exhibit a high content of fine sediments (mean d_{50} = 160 μm and mud content of 55%). During most of the year, this location coincides with the upstream end of the ETM, and the formation of bedforms is likely to be inhibited by the high mud content and the near-bed sediment-induced stratification (Baas et al., 2011; Becker et al., 2013). Downstream of Weser-km 74, the bedform fields that are observed are less extensive and with a smaller bedform density than in Bedform Field 1. This is in part due to the dredging activities which are taking place there (Figure 2c). Furthermore, the analysis presented here was carried out on a 200 m-wide portion of the bed situated in the centre of the navigation channel, whereas the main channel in the Outer Weser is much wider than that (Figure 2d). This is also where the estuary enters the North Sea, where a network of channels and intertidal flats develops. Therefore, dune fields in this area are not restrained to the (centre of the) navigation channel the results of our analysis may not be interpreted as representative of the whole outer estuary, where local spatial variations are likely to take place.

Interestingly, mean bedform height is only little affected by discharge (overall difference of around 3 cm between mean bedform height in times of high and low discharge), but the bedforms are on average 7 m longer in times of high discharge than in times of low discharge. Nasner (1974) analysed echosounder data collected between 1966 and 1972 in the Weser Estuary between Weser-km 18 and 59. He observed that bedform height varied inversely to river discharge, whereas bedform length did not vary much during the year. He argued that in times of high discharge, the ebb velocities increase due to the combined influence of river and tidal flows, which led to the erosion of the dune crests and a flattening of the bedforms. In times of low discharge, the dune crests are thought to rise due to sedimentation, until another new state of equilibrium is reached. Therefore, the results of the present study do not agree with Nasner's (1974) analysis. The exact dynamics which led to the observed results still need to be assessed in detail, which is beyond the reach of the present study.

Along Bedform Field 1, bedforms were observed to be more ebb-asymmetric in times of high discharge than in times of low discharge. This finding fits well with previous studies investigating bedform orientation and migration in estuaries, which showed that bedforms are more ebb-asymmetric in times of high discharge compared to times of low discharge (Nasner, 1974; Zorndt et al., 2011). Along Bedform Field 2, bedform asymmetry does not show clear changes between low and high discharge, and bedforms stay generally symmetric. Interestingly, along Bedform Field 3, the bedforms are more flood-asymmetric in times of high discharge than in times of low discharge, which contrasts with observations along Bedform Field 1. These differences may be explained by two main reasons. First, it can be due to localized spatial variations. Along Bedform Field 2, the estuary enters the North Sea, the navigation channel widens and several secondary channels are formed. Some channels become ebb-dominated and others flood-dominated. The present analysis was carried out only on

the middle of the navigation channel and certainly misses some local variations in bedform morphology. Second, it may be due to intensified estuarine circulation, which results in stronger flood-asymmetric bottom currents in times of high discharge compared to times of low discharge. Berne et al. (1993) observed bedforms in the Outer Gironde Estuary which were more flood-asymmetric in times of high discharge than in times of low discharge. Recently, van der Sande et al. (2021) showed, using a process-based modelling approach, that variations in gravitational estuarine circulation can induce ebb-oriented bedform migration during low discharge but flood-oriented migration during high discharge. They proposed that these processes are most likely to happen in the outer estuary, where there is a significant salinity gradient, a large depth and a small residual flow velocity. Therefore, it appears likely that gravitational estuarine circulation may be the cause of the change in bedform asymmetry, depending on discharge along Bedform Field 3, and this should be explored in detail.

4.2 | Comparison with bedforms in other estuaries and in rivers

The Weser bedforms are predominantly shorter in height and length (median depth/height = 10.9 and length/depth = 2.3) than the median relative height and length given by Bradley and Venditti (2017) (depth/height = 7.7 and length/depth = 5.9; see also Figures 5c and d and Supporting Information 2). It suggests that bedforms found in the Weser Estuary are smaller than bedforms in large rivers. This may be due to the difference in hydrodynamics: unidirectional currents in rivers, which have the potential to steadily mobilize sediment; and reversing currents in the Weser Estuary, where flow velocity is high enough to erode and transport sediment only during part of the tidal cycle, and where transport capacity is therefore reduced compared to rivers.

Cisneros et al. (2020) observed that dunes in some of the world's big rivers have low-angle lee side slopes, with average mean and maximum lee side angles of 13.4 and 20.5°. The bedforms observed in the Weser Estuary have, on average, mean lee side angles of 6.0° (ebb) and 4.6° (flood), and maximum lee side angles of 11.6° (ebb) and 10.0° (flood). It should be noted that Cisneros et al. (2020) analysed bathymetry with a much higher resolution (generally 0.5 m) than that available for the present observations (2 m), and may have been able to detect angles locally steeper than what was possible here. The bedform lee side slopes measured here compare well to those reported by Berne et al. (1993) in the Gironde Estuary, France, where the mean lee side slopes were reported to be 6.7 and 12.5°. Aliotta and Perillo (1987) observed that the lee slope of large bedforms in the entrance of the Bahia Blanca Estuary, Argentina, was on average 11°. However, comparison with previous studies is often complicated by the fact that it is unclear how exactly the lee slopes were defined: as the steepest portion of the lee side (i.e. similar to the maximum slope), or as the average slope between the crest and the trough (i.e. mean slope).

Cisneros et al. (2020) report that the majority of the maximum lee side slopes over dunes in large rivers are located in the lower half of the bedform lee side, close to the trough (average vertical position of the maximum angle at 0.3–0.4 between the trough and the crest). Furthermore, Lefebvre et al. (2016) found that bedforms from two large rivers had predominantly well-developed crestal platforms and a steep face (there defined as the portion of the lee side steeper than 10°) situated close to the bedform trough. In contrast, the average vertical position of the maximum angle for bedforms in the Weser Estuary was calculated to be at 0.60 (ebb) and 0.63 (flood) between the trough and the crest (i.e. in the upper half of the bedforms, near the crest). Furthermore, over bedforms which possess a steep face (i.e. bedforms with a portion of the lee side steeper than 15°), the steep face was also observed to be predominantly close to the crest, with horizontal positions from 0.1 to 0.4 between the crest and trough. In their review of estuarine bedforms, Dalrymple and Rhodes (1995) also noted that the steepest portion of estuarine bedforms was usually observed high on the lee side, with the lower lee side parts having much lower inclinations. Therefore, it appears that the shape of bedforms from large rivers is characterized by a relatively flat crest and steeper slope towards the trough, whereas estuarine bedforms have steeper slopes close to the crest, and flat troughs (Figure 9). This difference in morphology is likely due to the difference in hydrodynamic forcing. Fenster et al. (1990) suggested that large bedforms observed in Long Island Sound, USA, have concave-up slope because daily tidal current put in motion sand situated on the bedform crest, whereas the sediment in the trough was remobilized only during spring tide or when storm-generated currents were superimposed on the tidal flow. Dalrymple and Rhodes (1995) summarized that in estuaries where the currents are weak, concave sides and trochoidal profiles (i.e. the shape of the Weser bedforms in Figure 9b) are common because the threshold of sediment motion may not be exceeded for long periods, especially in the trough. Ernstsen et al. (2006a) showed, from high temporal and spatial measurements of bedform morphology in the Grådyb tidal inlet channel, Denmark, that sediment was actively moved at the crest during a tidal cycle, forming a 'flood cap', whereas the trough was relatively immobile. This flood cap was moved back and forth over the crest by the tidal flow. The presence of active sediment transport and superimposed bedform movement at the bedform crest, and low movement at the trough, is likely to be responsible for the bedform shape observed in the Weser Estuary, with a steep crest and flat trough (Figure 9e). In rivers, the sediment eroded from the crest is invariably being moved downstream, resulting in a flat crest and steep lower lee side (Figure 9d).

The bedforms in the Weser Estuary are generally 2D, with little variation of three-dimensionality along the estuary or with discharge. Rubin (2012) predicted theoretically that bedforms formed in tidal environments with ebb and flood currents showing similar velocities should be 2D and straight-crested. The present observation of bedforms in the Weser Estuary seems to agree with their hypothesis. However, no variation of the 3D properties is seen along the estuary, whereas tidal properties (velocity and duration of ebb and flood currents) are likely to vary. In contrast, the lack of variations may be due to the limited crosswise extent of this study (200 m) and the restriction to the main channel. Furthermore, there is currently no other datasets of 3D properties from natural bedform fields to which the 3D parameters calculated here could be compared. It would be beneficial to evaluate the 3D character of bedform fields as a function of flow properties in a wide variety of environments, as already argued by Rubin (2012). The present dataset constitutes a first step towards this goal.

4.3 | Implications for flow separation, turbulent wake and bedform roughness

Bedform morphology, and how it varies in time and space, has some strong implications in terms of the presence and size of flow separation, turbulent wake and bedform roughness. Herrling et al. (2021) recently argued that the contrasting effects of dune asymmetry on residual bed load transport may be of similar importance as the controls of seasonal variations of discharge on net sediment fluxes. Furthermore, recent studies (Kwoll et al., 2016; Lefebvre & Winter, 2016) have confirmed the early work of Ogink (1989), who suggested that bedform roughness is not only related to bedform height and length, but also to their lee side angle: bedforms with a steeper lee side produce more roughness than bedforms with a gentler lee side. Therefore, a correct description of bedform morphology, specifically the shape of their lee side(s), is needed in order to correctly estimate bedform roughness.

Since flow in the Weser Estuary is reversing, the position of the lee side compared to the current direction needs to be considered when relating bedform shape and roughness. For example, it is likely that a bedform with a steep flood lee side but a gentle ebb lee side will create roughness during the flood phase only (e.g. Figure 1, bottom left). Therefore, the present bedform morphology analysis is done in relation to the ebb and flood lee sides. The Weser bedforms are predominantly low-angle dunes, with mean lee side angles on average less than 10°, and maximum lee side angle on average lower than 15°. Lefebvre and Winter (2016) showed that a fully grown flow separation and turbulent wake, creating a strong roughness, forms over bedforms with a slope of 24°. Of all the measured bedforms, only 0.01% (flood) and 2.1% (ebb) have a maximum lee side angle of 24° or more. This suggests that only very few bedforms have the potential to produce a fully developed flow separation and create high roughness. However, it may be that, following grain roughness definition (e.g. Van Rijn, 1993), and as hypothesized by Van Der Mark et al. (2008), bedform roughness from a natural bedform field may be related to the 90th percentile of mean or maximum lee side angle rather than to the average lee side angles. This hypothesis still needs to be tested.

Lefebvre (2019) observed from numerical modelling results above a natural bedform field that bedforms which possess a steep face (portion of the lee side steeper than 15°) are steep enough to initiate flow separation and produce a turbulent wake. They suggested that these bedforms have the potential to generate bedform roughness. A significant number of bedforms possess a steep face: 30% of all the measured bedforms have an ebb steep face, and 11% have a flood steep face (see Supporting Information 2).

In order to assess the potential for flow separation and turbulent wake production over a natural bedform field, we assume that a flow separation and strong turbulent wake will form over steep faces and that this will produce bedform roughness. The area of steep faces per square kilometre, or steep face area density, is used here as an indicator of the potential for flow separation and turbulent wake production along the Weser Estuary. It was calculated during the ebb and flood, and in times of high and low discharge (Figure 10). During the flood in times of high discharge, the bedforms are likely to create no to very little flow separation, wake and roughness. During the ebb, however, the bedforms between Weser-km 20 and 55 have the potential to produce flow separation, wake and roughness. In times of low discharge, flow separation, wake and roughness may be high between Weser-km 20 and 35 during the flood and between Weser-km 20 and 55 during the ebb.

Although steep face density may only qualitatively indicate the potential for flow separation, turbulence production and bedform roughness, its variations in time and space along the estuary have

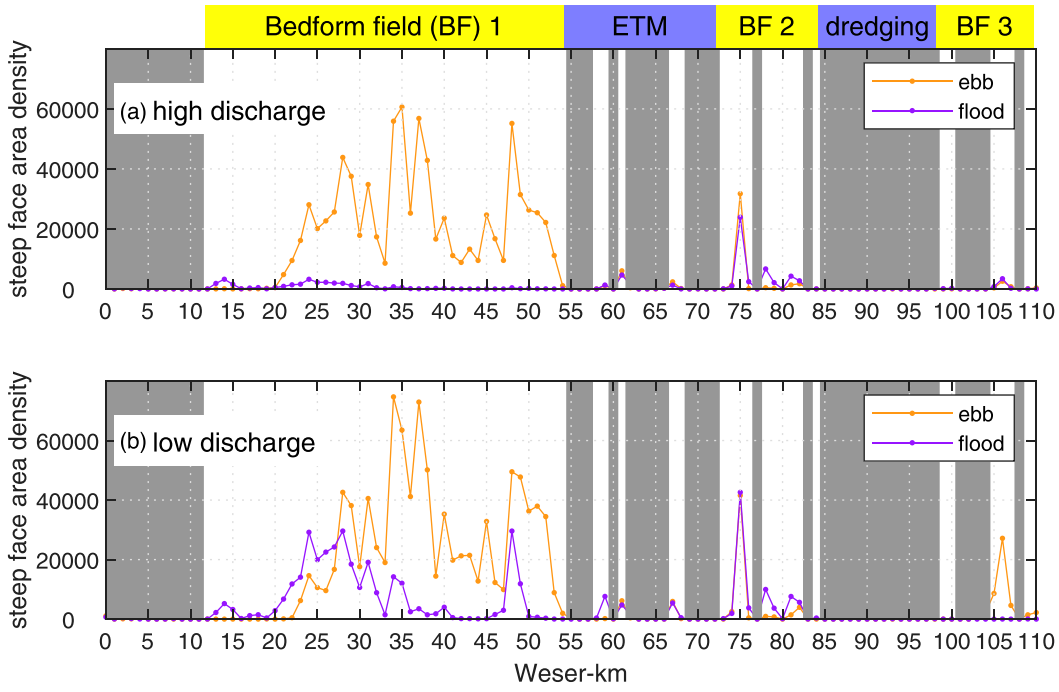

FIGURE 10 Steep face-area density during the ebb and flood and in times of low and high discharge. The steep face density is used as an indicator of flow separation, turbulent wake and roughness production over a bedform field

important implications in terms of the parameterization of bedform roughness in numerical models. It shows in particular that bedform roughness is likely to vary spatially depending on bedform properties (especially steep face presence and height), but also on short timescales during ebb and flood, and on longer timescales depending on discharge and adaptation of bedforms to hydrodynamic parameters.

5 | CONCLUSIONS

A large dataset of monthly bathymetry measured along the Weser Estuary over a 5-year period was analysed to detect and characterize bedforms. Bedform properties, with a focus on bedform shape, were calculated. Several results were observed:

1. Bedform properties vary spatially and temporally along the estuary. Along the main bedform field (Weser-km 12 to 55), bedforms are mostly flood-asymmetric in the upstream part, gradually becoming symmetrical then ebb-asymmetric in the downstream part of the bedform field. In times of high discharge, bedforms in this bedform field are more ebb-asymmetric than in times of low discharge.
2. Bedforms in the Weser Estuary are predominantly low-angle dunes with their steepest slope situated near the bedform crest. This contrasts with low-angle dunes in large rivers which have their steepest slope close to the trough. The shape of the Weser bedforms is likely due to the action of reversing tidal currents which mobilizes sediment principally at the crest, creating a steep slope there.
3. The Weser bedforms are generally 2D, with little variation of three-dimensionality in time or space. More measurements of bedform three-dimensionality in rivers and tidal environments are needed to assert a trend between three-dimensionality and hydrodynamic forcing.
4. Although the Weser bedforms are mainly low-angle, a significant proportion of bedforms (one-third during the ebb and one-tenth during the flood) possesses a steep face (portion of the lee side with a slope steeper than 15°). These bedforms are likely to create flow separation and a turbulent wake and have a strong potential to induce bed roughness. The steep face area density varies spatially along the estuary as a function of the tidal phase (ebb and flood), but also depending on discharge.

The results presented here are important in terms of characterizing bedform dynamics in tidal environments. The shape of bedforms has until now received little attention, while it is likely to play an important role in the interaction between hydrodynamics, sediment movement and geomorphology.

ACKNOWLEDGEMENTS

Alice Lefebvre was funded by the German Research Foundation (Deutsche Forschungsgemeinschaft, DFG), Project 345915838, during most of this research, and is now funded through the Cluster of Excellence 'The Ocean Floor – Earth's Uncharted Interface'. Gerald Herrling is funded by the research project FAUST, financed by and conducted in cooperation with the German Federal Waterways Engineering and Research Institute (BAW). The Weser–Jade–Nordsee Waterways and Shipping Authorities in Bremerhaven are greatly thanked for providing the gridded bathymetries. The insightful comments of two reviewers and the associate editor greatly helped in improving the manuscript, we would like to thank them for their time.

AUTHOR CONTRIBUTIONS

Conceptualization of the required analysis was made through collegial discussion between all co-authors. Alice Lefebvre developed the methodology and analysed the data, which were discussed at an early stage with all co-authors. Alice Lefebvre wrote the manuscript (with in-depth discussions with Gerald Herrling), which was reviewed and commented on by all co-authors.

DATA AVAILABILITY STATEMENT

Results are available through the Publishing Network for Geoscientific & Environmental Data (PANGAEA, https://doi.org/10.1594/PANGAEA.936104). The codes to analyse the data have been made available (https://github.com/DrAliceLefebvre/Weser_Bedform_Analysis_Codes).

ORCID

Alice Lefebvre https://orcid.org/0000-0002-9234-8279
Gerald Herrling https://orcid.org/0000-0003-0530-8752
Marius Becker https://orcid.org/0000-0001-5469-2506
Knut Krämer https://orcid.org/0000-0002-4259-3989
Christian Winter https://orcid.org/0000-0002-8043-2131

REFERENCES

Aliotta, S. & Perillo, G.M.E. (1987) A sand wave field in the entrance to Bahia Blanca Estuary, Argentina. *Marine Geology*, 76, 1–14. https://doi.org/10.1016/0025-3227(87)90013-2

Allen, J.R.L. (1968) *Current Ripples*. New York: Elsevier.

Baas, J.H., Best, J.L. & Peakall, J. (2011) Depositional processes, bedform development and hybrid bed formation in rapidly decelerated cohesive (mud–sand) sediment flows. *Sedimentology*, 58(7), 1953–1987. https://doi.org/10.1111/j.1365-3091.2011.01247.x

Barnard, P.L., Erikson, L.H. & Kvitek, R.G. (2011) Small-scale sediment transport patterns and bedform morphodynamics: New insights from high-resolution multibeam bathymetry. *Geo-Marine Letters*, 31(4), 227–236. https://doi.org/10.1007/s00367-011-0227-1

Becker, M., Schrottke, K., Bartholomä, A., Ernstsen, V., Winter, C. & Hebbeln, D. (2013) Formation and entrainment of fluid mud layers in troughs of subtidal dunes in an estuarine turbidity zone. *Journal of Geophysical Research: Oceans*, 118(4), 2175–2187. https://doi.org/10.1002/jgrc.20153

Berne, S., Castaing, P., Le Drezen, E. & Lericolais, G. (1993) Morphology, internal structure, and reversal of asymmetry of large subtidal dunes in the entrance to Gironde Estuary (France). *Journal of Sedimentary Research*, 63, 780–793. https://doi.org/10.1306/D4267C03-2B26-11D7-8648000102C1865D

Best, J. (2005) The fluid dynamics of river dunes: A review and some future research directions. *Journal of Geophysical Research*, 110(F4), 21. https://doi.org/10.1029/2004JF000218

Bradley, R.W. & Venditti, J.G. (2017) Reevaluating dune scaling relations. *Earth-Science Reviews*, 165, 356–376. https://doi.org/10.1016/j.earscirev.2016.11.004

Cisneros, J., Best, J., van Dijk, T., de Almeida, R.P., Amsler, M., Boldt, J., *et al*. (2020) Dunes in the world's big rivers are characterized by low-angle lee-side slopes and a complex shape. *Nature Geoscience*, 13(2), 156–162. https://doi.org/10.1038/s41561-019-0511-7

Dalrymple, R.W. & Rhodes, R.N. (1995) Estuarine dunes and bars. In: Perillo, G.M.E. (Ed.) *Developments in Sedimentology*. Amsterdam: Elsevier, pp. 359–422.

Ernstsen, V.B., Noormets, R., Hebbeln, D., Bartholomä, A. & Flemming, B. W. (2006a) Precision of high-resolution multibeam echo sounding coupled with high-accuracy positioning in a shallow water coastal environment. *Geo-Marine Letters*, 26(3), 141–149. https://doi.org/10.1007/s00367-006-0025-3

Ernstsen, V.B., Noormets, R., Winter, C., Hebbeln, D., Bartholomä, A., Flemming, B.W. & Bartholdy, J. (2006b) Quantification of dune dynamics during a tidal cycle in an inlet channel of the Danish Wadden Sea. *Geo-Marine Letters*, 26(3), 151–163. https://doi.org/10.1007/s00367-006-0026-2

Federal Waterway Network. (n.d.) Online resource. https://atlas.wsv.bund.de/bwastr-locator/client/

Fenster, M.S., Fitzgerald, D.M., Bohlen, W.F., Lewis, R.S. & Baldwin, C.T. (1990) Stability of giant sand waves in eastern Long Island Sound, U.S.A. *Marine Geology*, 91(3), 207–225. https://doi.org/10.1016/0025-3227(90)90037-K

Flussgebietsgemeinschaft Weser (n.d.) Online resource. https://datenbank.fgg-weser.de/weserdatenbank/#/

Franzius, L. (1888). Die Korrektion der Unterweser: auf Veranlassung der Bremischen Deputation für die Unterweserkorrektion, Bremen. https://brema.suub.uni-bremen.de/content/titleinfo/1490943

Grabemann, I. & Krause, G. (2001) On different time scales of suspended matter dynamics in the Weser Estuary. *Estuaries*, 24(5), 688–698. https://doi.org/10.2307/1352877

Grabemann, I., Uncles, R.J., Krause, G. & Stephens, J.A. (1997) Behaviour of turbidity maxima in the Tamar (U.K.) and Weser (F.R.G.) estuaries. *Estuarine, Coastal and Shelf Science*, 45(2), 235–246. https://doi.org/10.1006/ecss.1996.0178

Harris, P.T. & Collins, M.B. (1984) Bedform distributions and sediment transport paths in the Bristol Channel and Severn Estuary, U.K. *Marine Geology*, 62(1–2), 153–166. https://doi.org/10.1016/0025-3227(84)90059-8

Herrling, G., Becker, M., Lefebvre, A., Zorndt, A., Krämer, K. & Winter, C. (2021) The effect of asymmetric dune roughness on tidal asymmetry in the Weser Estuary. *Earth Surface Processes and Landforms*, 46(11), 1–18. https://doi.org/10.1002/esp.5170

Kubicki, A., Kösters, F. & Bartholomä, A. (2017) Dune convergence/divergence controlled by residual current vortices in the Jade tidal channel, south-eastern North Sea. *Geo-Marine Letters*, 37(1), 47–58. https://doi.org/10.1007/s00367-016-0470-6

Kunz, H. (1994) Salinity and water levels in the Weser Estuary during the last hundred years: Anthropogenic influences on the coastal environment. In: Edge, B.L. (Ed.) *Proceedings of the 24th International Conference on Coastal Engineering*. Reston, VA: American Society of Civil Engineers.

Kwoll, E., Venditti, J.G., Bradley, R.W. & Winter, C. (2016) Flow structure and resistance over subaquaeous high- and low-angle dunes. *Journal of Geophysical Research – Earth Surface*, 121(3), 545–564. https://doi.org/10.1002/2015JF003637

Lefebvre, A. (2019) Three-dimensional flow above river bedforms: Insights from numerical modeling of a natural dune field (Río Paraná, Argentina). *Journal of Geophysical Research – Earth Surface*, 124(8), 2241–2264. https://doi.org/10.1029/2018jf004928

Lefebvre, A., Paarlberg, A.J. & Winter, C. (2016) Characterising natural bedform morphology and its influence on flow. *Geo-Marine Letters*, 36(5), 379–393. https://doi.org/10.1007/s00367-016-0455-5

Lefebvre, A. & Winter, C. (2016) Predicting bed form roughness: The influence of lee side angle. *Geo-Marine Letters*, 36(2), 121–133. https://doi.org/10.1007/s00367-016-0436-8

Maddux, T.B., Nelson, J.M. & McLean, S.R. (2003) Turbulent flow over three-dimensional dunes: 1. Free surface and flow response. *Journal of Geophysical Research – Earth Surface*, 108(F1), 6009. https://doi.org/10.1029/2003JF000017

Nasner, H. (1974) Prediction of the height of tidal dunes in estuaries. *Coastal Engineering*, 1974, 1036–1050. https://doi.org/10.1061/9780872621138.063

Nasner, H., Pieper, R. & Torn, P. (2009) Dredging of tidal dunes. In: Smith, J.M.K. (Ed.) *Proceedings of Coastal Engineering 2008*. Singapore: World Scientific, pp. 2761–2773.

Ogink, H. (1989) *Hydraulic Roughness of Single and Compound Bed Forms, part XI. Report on Model Investigations*. Delft: Delft Hydraulics Laboratory.

Ogor, J. (2018). Design of algorithms for the automatic characterization of marine dune morphology and dynamics. PhD thesis, ENSTA Bretagne – École nationale supérieure de techniques avancée.

Parsons, D.R., Best, J.L., Orfeo, O., Hardy, R.J., Kostaschuk, R. & Lane, S.N. (2005) Morphology and flow fields of three-dimensional dunes, Rio Paraná, Argentina: Results from simultaneous multibeam echo sounding and acoustic Doppler current profiling. *Journal of Geophysical Research*, 110(F4), F04S03. https://doi.org/10.1029/2004JF000231

Rubin, D.M. (2012) A unifying model for planform straightness of ripples and dunes in air and water. *Earth-Science Reviews*, 113(3–4), 176–185. https://doi.org/10.1016/j.earscirev.2012.03.010

Scheiber, L., Lojek, O., Götschenberg, A., Visscher, J. & Schlurmann, T. (2021) Robust methods for the decomposition and interpretation of compound dunes applied to a complex hydromorphological setting. *Earth Surface Processes and Landforms*, 46(2), 478–489. https://doi.org/10.1002/esp.5040

Southard, J.B. & Boguchwal, L.A. (1990) Bed configuration in steady unidirectional water flows; Part 2. Synthesis of flume data. *Journal of Sedimentary Research*, 60(5), 658–679. https://doi.org/10.1306/212F9241-2B24-11D7-8648000102C1865D

Van Der Mark, C.F., Blom, A. & Hulsher, S.J.M.H. (2008) Quantification of variability in bedform geometry. *Journal of Geophysical Research*, 113(F3), F03020. https://doi.org/10.1029/2007JF000940

Van Der Sande, W.M., Roos, P.C., Gerkema, T. & Hulscher, S.J.M.H. (2021) Gravitational circulation as driver of upstream migration of estuarine sand dunes. *Geophysical Research Letters*, 48, e2021GL093337. https://doi.org/10.1029/2021GL093337

Van Rijn, L.C. (1984) Sediment transport, Part III: Bed forms and alluvial roughness. *Journal of Hydraulic Engineering*, 110(12), 1733–1754. https://doi.org/10.1061/(ASCE)0733-9429(1984)110:12(1733)

Van Rijn, L.C. (1993) *Principles of Sediment Transport in Rivers, Estuaries and Coastal Seas*. Amsterdam: Aqua Publications.

Venditti, J.G. (2007) Turbulent flow and drag over fixed two- and three-dimensional dunes. *Journal of Geophysical Research*, 112(F4), F04008. https://doi.org/10.1029/2006JF000650

Venditti, J.G. (2013) Bedforms in sand-bedded rivers. In: Shroder, J. & Wohl, E. (Eds.) *Treatise on Geomorphology*. San Diego, CA: Academic Press, pp. 137–162.

Wang, L., Yu, Q., Zhang, Y.Z., Flemming, B.W., Wang, Y.W. & Gao, S. (2020) An automated procedure to calculate the morphological parameters of superimposed rhythmic bedforms. *Earth Surface Processes and Landforms*, 45(14), 3496–3509. https://doi.org/10.1002/esp.4983

Zorndt, A. & Schlurmann, T. (2014) Investigating impacts of climate change on the Weser Estuary. *Die Küste*, 81, 541–550.

Zorndt, A.C., Wurpts, A. & Schlurmann, T. (2011) The influence of hydrodynamic boundary conditions on characteristics, migration, and associated sand transport of sand dunes in a tidal environment. *Ocean Dynamics*, 61(10), 1629–1644. https://doi.org/10.1007/s10236-011-0452-1

SUPPORTING INFORMATION

Additional supporting information may be found in the online version of the article at the publisher's website.

How to cite this article: Lefebvre, A., Herrling, G., Becker, M., Zorndt, A., Krämer, K. & Winter, C. (2021) Morphology of estuarine bedforms, Weser Estuary, Germany. *Earth Surface Processes and Landforms*, 1–15. Available from: https://doi.org/10.1002/esp.5243